

See discussions, stats, and author profiles for this publication at: <https://www.researchgate.net/publication/239377248>

# Leaching of Malachite Ore in $\text{NH}_3$ Saturated Water

ARTICLE in INDUSTRIAL & ENGINEERING CHEMISTRY RESEARCH · JULY 2004

Impact Factor: 2.59 · DOI: 10.1021/ie0342558

CITATIONS

18

READS

25

## 3 AUTHORS:



Mehmet Arzutug

Ataturk University

7 PUBLICATIONS 71 CITATIONS

SEE PROFILE



Mehmet Muhtar Kocakerim

Çankırı Karatekin Üniversitesi

68 PUBLICATIONS 1,129 CITATIONS

SEE PROFILE



Mehmet Çopur

Bursa Teknik Üniversitesi

37 PUBLICATIONS 553 CITATIONS

SEE PROFILE

# Leaching of Malachite Ore in $\text{NH}_3$ -Saturated Water

M. Emin Arzutug,\* M. Muhtar Kocakerim, and M. Copur

*Kimya Mühendisliği Bölümü, Atatürk Üniversitesi Mühendislik Fakültesi, 25240-Erzurum, Türkiye*

In this study, the leaching kinetics of malachite  $[\text{CuCO}_3 \cdot \text{Cu}(\text{OH})_2]$ , an oxidized copper ore, was investigated in water saturated with ammonia gas. In the experiments, the ammonia concentration of the solution, the particle size of the ore, the temperature, the stirring speed, and the solid-to-liquid ratio were chosen as parameters. It was determined that the leaching rate of malachite increased with decreasing particle size and solid-to-liquid ratio and increasing reaction temperature, ammonia concentration, and stirring speed. The leaching kinetics was examined by statistical methods applied to the experimental data. It was found that the leaching rate fitted a pseudo-second-order kinetic model with an activation energy of  $85.16 \text{ kJ} \cdot \text{mol}^{-1}$ .

## 1. Introduction

Copper is known as one of the metals used most commonly in the world. This situation has led to the development of more economical methods of copper production. Copper is used mostly in the electrical and electronics industries because of its high conductivity. Its second highest consumption area is the rolling industry. In addition, copper and its alloys are used in the electrotechnic, engine, communication, and aviation industries, for electricity production and distribution, in measurement devices, in the chemical industry, etc.

Copper generally is found in nature in the form of sulfide and oxide minerals, such as malachite  $[\text{CuCO}_3 \cdot \text{Cu}(\text{OH})_2]$ , azurite  $[2\text{CuCO}_3 \cdot \text{Cu}(\text{OH})_2]$ , chalcocite  $(\text{Cu}_2\text{O})$ , and bornite  $(\text{Cu}_5\text{FeS}_4)$ . Metallic copper is produced from these ores by pyrometallurgical and hydrometallurgical methods.

Hydrometallurgical methods of processing ores or their concentrates have an increasing importance in the extraction of nonferrous metals. The development of copper ore processing methods has led to the progress of extraction methods in copper recovery from ammoniacal leaching solutions.<sup>1</sup> Hydrometallurgical processes are preferred for the recovery of copper from oxidized copper ores because the application of pyrometallurgical methods to these kinds of ores is more difficult. Then, copper in the leaching solutions is recovered by electrolysis or cementation. In these processes, sulfuric acid solutions are generally used as the leaching agent.<sup>2</sup>

Nevertheless, ammonia–ammonium carbonate/sulfate leaching systems have some advantages over acid leaching systems. Some solvents, called lixiviants, are selective for the heavy metals rather than light metals such as aluminum and calcium. These lixiviants can be essentially easily regenerated.<sup>3</sup> The use of lixiviants is an attractive alternative for the purification of loaded solutions to give a copper-rich solution for electrolytic recovery and production of high-grade copper. In these applications, copper in leaching solutions can be selectively extracted into a kerosene solution containing a copper-selective reagent (e.g., Lix 63, Lix 64, Lix 984N, M5640). The copper can be stripped from the organic

solution to a new aqueous solution to obtain a copper-rich solution.<sup>4</sup> Then, pure copper can be obtained from this solution by electrowinning or cementation.

Ores containing oxidized copper minerals such as tenorite, malachite, or azurite are readily leached by ammonia–ammonium carbonate solutions. This technique is particularly fruitful when these minerals occur in high-limestone gangue.

Awakura et al. studied the dissolution of malachite in aqueous EDTA solutions and assumed a mechanism involving the Langmuir-type adsorption of EDTA. They claimed that the dissolution rate of malachite was controlled by the removal of  $\text{Cu}(\text{II})$ -EDTA complex from the malachite lattice. The authors found varying values of the activation energy, ranging from  $51.4$  to  $57.5 \text{ kJ} \cdot \text{mol}^{-1}$  for different pHs.<sup>5</sup>

Çolak et al. investigated the dissolution of malachite in water saturated with sulfur dioxide and determined that the activation energy was  $32.12 \text{ kJ} \cdot \text{mol}^{-1}$  and that the process was controlled by chemical reaction.<sup>6</sup> Yartaşı and Çopur studied the dissolution kinetics of malachite in ammonium chloride solutions and found a mathematical model for the dissolution process. An activation energy of  $81.3 \text{ kJ} \cdot \text{mol}^{-1}$  was determined for this process in which the dissolution rate was controlled by diffusion through the product film.<sup>7</sup>

Künkül et al. examined the dissolution of malachite in ammonia solutions and proposed a mathematical model for the process kinetics. They declared that the activation energy was  $22.338 \text{ kJ} \cdot \text{mol}^{-1}$  for this process, controlled by diffusion through the ash film.<sup>8</sup> Oudenne and Olson reported that the leaching of malachite with ammonium carbonate took place in two stages. At the first stage, the initial dissolution of malachite proceeded rapidly, but after about 10% of the reaction, the rate was reduced by surface blockage due to the presence of a needle-structured intermediate, presumably  $\text{Cu}(\text{OH})_2$ . The activation energy was  $64 \text{ kJ} \cdot \text{mol}^{-1}$  for stage I and  $75 \text{ kJ} \cdot \text{mol}^{-1}$  for stage II.<sup>9</sup> Konishi et al. studied the leaching kinetics of copper from natural chalcocite in basic  $\text{Na}_4\text{EDTA}$  solutions and observed that the effects of relevant operating variables on the dissolution rate were consistent with a kinetic model for electrochemical reaction control.<sup>10</sup> Ekmekyapar et al.<sup>11</sup> suggested that a semiempirical model for the dissolution kinetics of malachite and calculated the activation energy for the dissolution reaction as  $71 \text{ kJ} \cdot \text{mol}^{-1}$ .

\* To whom correspondence should be addressed. Tel.: (+90)-442-2314559. Fax: (+90)442-2360957. E-mail: arzutug@atauni.edu.tr.

**Table 1. Wet Chemical Analysis of the Ore Used in the Study**

component	content (%)
CuO	15.94
Fe <sub>2</sub> O <sub>3</sub>	6.20
Al <sub>2</sub> O <sub>3</sub>	0.48
Mn <sub>2</sub> O <sub>3</sub>	1.20
CaO	4.24
MgO	0.34
Na <sub>2</sub> O	0.04
K <sub>2</sub> O	0.05
SiO <sub>2</sub>	49.80
TiO <sub>2</sub>	0.30
P <sub>2</sub> O <sub>5</sub>	0.06
ZnO	7.61
SO <sub>2</sub>	0.48
others (TiO <sub>2</sub> , Cr <sub>2</sub> O <sub>3</sub> , MnO <sub>2</sub> , etc.)	0.15
loss at red heat (1000 °C)	13.11
total	100.00

The dissolution kinetics of an oxidized copper ore, primarily malachite, in water saturated with chlorine and in H<sub>2</sub>SO<sub>4</sub> solutions was studied.<sup>12,13</sup> A kinetic model of the dissolution of copper(II) oxide in EDTA solutions was proposed, and the effects of pH and the EDTA concentration was investigated in the experiments.<sup>14</sup>

In the present study, the leaching kinetics of malachite ore in NH<sub>3</sub>-saturated water were investigated, using the parameters temperature, NH<sub>3</sub> concentration in solution, solid-to-liquid ratio, particle size, and stirring speed.

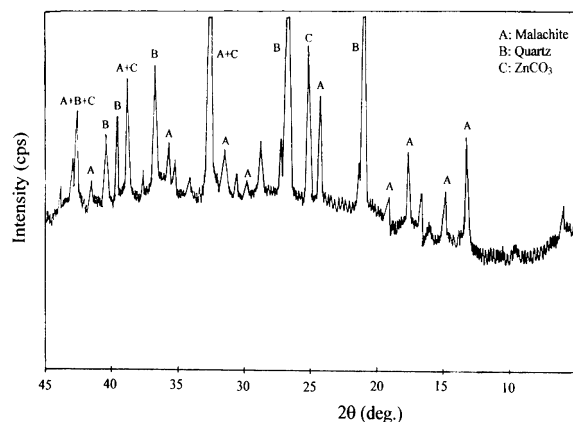
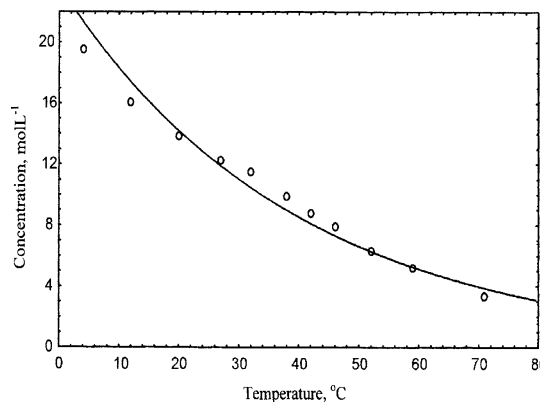
## 2. Experimental Section

**2.1. Preparation of Materials.** The sample, which was provided from the mines in Tunceli, Turkey, was crushed, ground, and separated to fractions of +1180–1400, +710–850, +355–425, +180–212, and +75–90  $\mu\text{m}$  using ASTM standard sieves. The chemical analysis results of the ore given in Table 1 show that the ore contains 15.94% CuO. An X-ray diffractogram of the original sample obtained on a Rigaku DMAX 2000 series X-ray diffractometer is shown in Figure 1. It is seen that the sample contains essentially malachite, quartz, and zinc carbonate. Ammonia gas was obtained from Turkish Nitrogen Industry in Kütahya, Turkey, with a purity of 99.5%. Ammonia gas is very soluble in water with a large solution heat, and its solubility decreases with increasing temperature.

To find the solubility of ammonia in water at various temperatures, 100 mL of distilled water was taken into a 250-mL flask, and its temperature was adjusted to the desired value by using a constant-temperature bath. NH<sub>3</sub> gas was then passed through it at a 7 L h<sup>-1</sup> flow rate under continuous stirring for a 1-h period accepted to be sufficiently to obtain an ammonia-saturated aqueous solution. Five milliliters of this solution was added to 25 mL of 0.5 M HCl solution (excess amount of HCl). The excess of amount the acid was titrated by 0.5 M NaOH solution, the amount of dissolved NH<sub>3</sub> was calculated for each temperature, and the solubility graph under 610 mmHg atmospheric pressure of Erzurum, Turkey, was plotted as in Figure 2.

**2.2. Method.** In the experiments, the ammonia gas concentration in the solution, the particle size, the reaction temperature, the stirring speed, and the solid-to-liquid ratio were chosen as parameters.

The leaching experiments were carried out in a 250-mL glass reactor, equipped with gas inlet and outlet tubes. The reactor was immersed in a circulating distilled water bath whose temperature was kept con-

**Figure 1.** X-ray diffractogram of malachite ore.**Figure 2.** Solubility of NH<sub>3</sub> in water as a function of temperature at 610 mmHg.

stant within  $\pm 0.10$  °C of the desired temperature by a constant-temperature circulator, Haake model E52. The reactor contents were mixed by a mechanical stirrer having a digital tachometer for measuring and controlling the stirring speed.

Before each experiment, 100 mL of distilled water was added into the reactor and then saturated with ammonia gas at atmospheric pressure. To study the effect of the NH<sub>3</sub> concentration on the leaching rate at constant temperature, NH<sub>3</sub> and N<sub>2</sub> gases were mixed at various ratios in a column that was filled with inert filling materials, and then this gas mixture was passed through the water in the reactor at a constant total volumetric rate.

After the reactive solution had been prepared, a certain amount of the sample was added into the reactor. During the reaction period, NH<sub>3</sub> or an NH<sub>3</sub>–N<sub>2</sub> mixture was passed continuously through the reaction medium. After each experiment, the reactor contents were filtered, and the amount of Cu<sup>2+</sup> in the filtrate was analyzed volumetrically.<sup>15</sup> The dissolution fraction of copper was calculated as follows

leached fraction of copper ( $X$ ) =

$$\frac{\text{amount of Cu}^{2+} \text{ passing to the solution}}{\text{amount of Cu}^{2+} \text{ in the original sample}}$$

The results were plotted as the dissolution fraction of copper ( $X$ ) versus time (Figures 3–7).

## 3. Results and Discussion

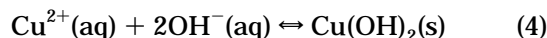
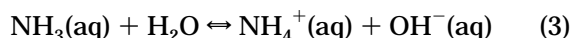
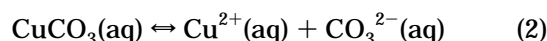
NH<sub>3</sub> is a weak base and also forms complexes with Cu<sup>2+</sup> in aqueous solutions. When the pH is kept within

a specified range, all of the  $\text{Cu}^{2+}$  in the solution can be in the form of water-soluble complexes.

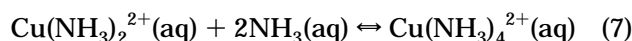
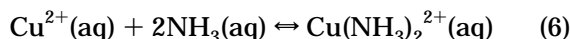
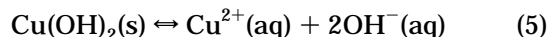
The thermodynamic behavior of a leaching system is presented on a potential–pH diagram, which shows the formation of domains within each of which a particular species is thermodynamically stable. The potential–pH diagram for the  $\text{Cu-NH}_3\text{-H}_2\text{O}$  system at 25 °C shows the extensions of the dissolution domains brought about by the formation of water-soluble copper amines; the largest areas belong to first  $\text{Cu}(\text{NH}_3)_4^{2+}$  and second  $\text{Cu}(\text{NH}_3)_2^{2+}$  for the pH range of the present system.<sup>4,8</sup>

Because pH values change between 11.8 and 12.1 within the chosen  $\text{NH}_3$  concentration range for the present work, copper is mainly in the form of  $\text{Cu}(\text{NH}_3)_4^{2+}$  complex, and no precipitation of any copper compound occurs under these conditions.

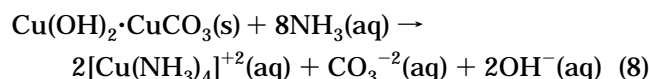
Assuming that the copper in the ore is in the form of  $\text{Cu}(\text{OH})_2\cdot\text{CuCO}_3$ , it was reported that  $\text{CuCO}_3$  is first dissolved to produce  $\text{Cu}(\text{OH})_2$  through the following reactions<sup>9</sup>



and then the following reactions take place



It is reported that the  $\text{Cu}(\text{NH}_3)_2^{2+}$  formed during the reaction is an intermediate and, at the end, it converts to the  $\text{Cu}(\text{NH}_3)_4^{2+}$  complex. The overall reaction for the leaching can be written as



**3.1. Effect of Particle Size.** The effect of particle size on the reaction rate was studied by performing the experiments using the fractions +1180–1400, +710–850, +355–425, +180–212, +75–90  $\mu\text{m}$  at 45 °C. These experiments were carried out at the ammonia concentration of 7.68  $\text{mol}\cdot\text{L}^{-1}$ , the solid-to-liquid ratio of 2/100  $\text{g}\cdot\text{mL}^{-1}$ , and the stirring speed of 400 rpm. As can be seen in Figure 3, the leaching rate increased as the particle size decreased. This case can be attributed to the increase in the number of particles per unit of solid weight; that is, the increase in the surface area causes better exposure of the copper ores to the solution with decreasing the particle size.

**3.2. Effect of Ammonia Concentration.** The effect of the ammonia concentration was investigated for the ammonia concentrations of 3.03, 3.54, 4.80, and 7.68  $\text{mol}\cdot\text{L}^{-1}$  at 45 °C. In the experiments, the particle size of +1180–1400  $\mu\text{m}$  was used with the solid-to-liquid ratio of 2/100  $\text{g}\cdot\text{mL}^{-1}$  and the stirring speed of 400 rpm. As seen in Figure 4, the leaching rate increased as the ammonia concentration increased.

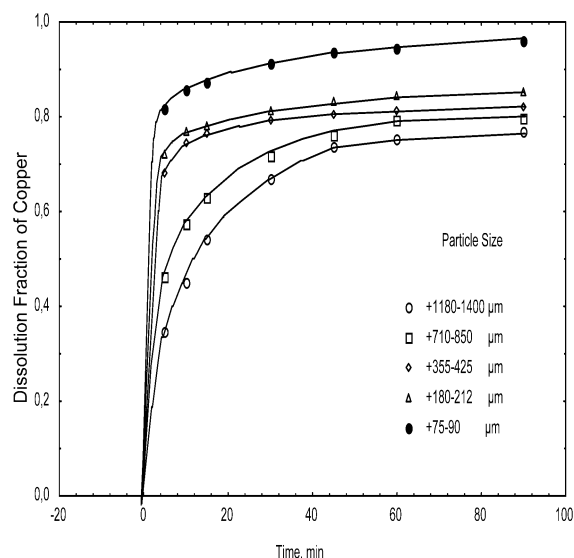


**Figure 3.** Effect of malachite particle size on the leaching rate in water saturated with  $\text{NH}_3$  gas ( $T = 45\text{ }^\circ\text{C}$ ,  $C = 7.68\text{ mol}\cdot\text{L}^{-1}$ ,  $S/L = 2/100\text{ g}\cdot\text{mL}^{-1}$ ,  $SS = 400\text{ rpm}$ ).

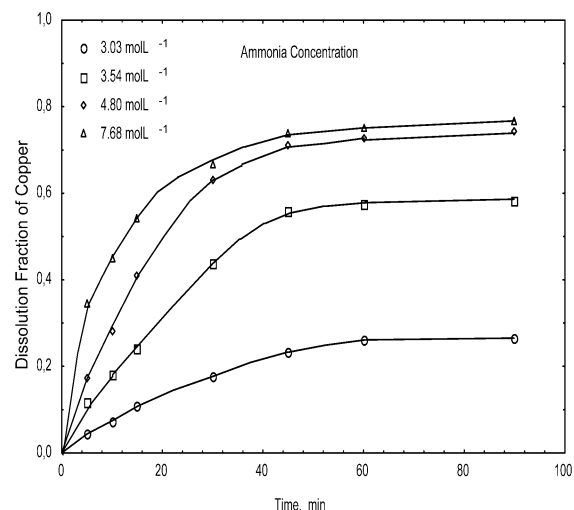


**Figure 4.** Effect of ammonia concentration on the leaching rate of malachite in water saturated with an  $\text{NH}_3\text{-N}_2$  gas mixture ( $D = +1180\text{--}1400\text{ }\mu\text{m}$ ,  $T = 45\text{ }^\circ\text{C}$ ,  $S/L = 2/100\text{ g}\cdot\text{mL}^{-1}$ ,  $SS = 400\text{ rpm}$ ).

**3.3. Effect of Solid-to-Liquid Ratio.** The effect of the solid-to-liquid ratio was studied for the ratios of 1/100, 2/100, 4/100, and 10/100  $\text{g}\cdot\text{mL}^{-1}$  at 45 °C. In the experiments, the ammonia concentration was 7.68  $\text{mol}\cdot\text{L}^{-1}$ , the particle size was +1180–1400  $\mu\text{m}$ , and the stirring speed was 400 rpm. Figure 5 shows that the leaching rate increased as the solid-to-liquid ratio decreased. This finding can be explained by the decrease in the amount of leaching reactant per unit amount of the solid with the increase of the solid-to-liquid ratio.

**3.4. Effect of Reaction Temperature.** The effect of reaction temperature was investigated for the temperatures of 4, 13, 21, 27, 34, and 45 °C. These experiments were carried out at the particle size fraction of +1180–1400  $\mu\text{m}$ , the ammonia concentration of 7.68  $\text{mol}\cdot\text{L}^{-1}$ , the solid-to-liquid ratio of 2/100  $\text{g}\cdot\text{mL}^{-1}$ , and the stirring speed of 400 rpm. The leaching rate of the ore increased as the reaction temperature increased, as seen in Figure 6.

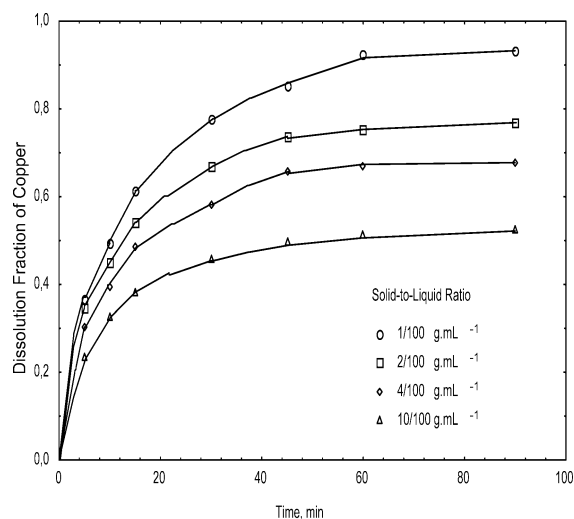


**Figure 5.** Effect of solid-to-liquid ratio on the leaching rate of malachite in water saturated with  $\text{NH}_3$  gas ( $D = +1180\text{--}1400\ \mu\text{m}$ ,  $T = 45\ ^\circ\text{C}$ ,  $C = 7.68\ \text{mol}\cdot\text{L}^{-1}$ ,  $\text{SS} = 400\ \text{rpm}$ ).

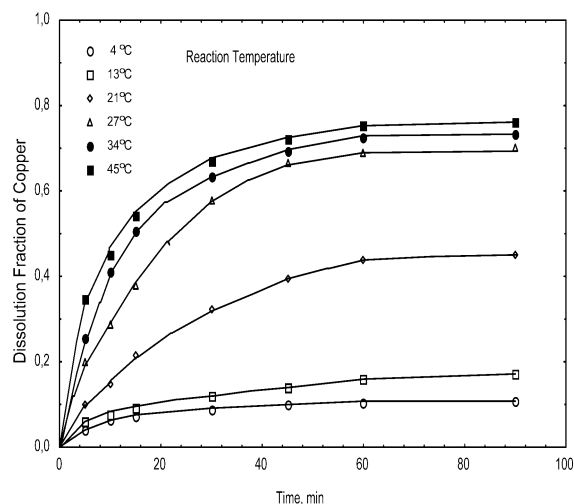


**Figure 6.** Effect of temperature on the leaching rate of malachite in water saturated with  $\text{NH}_3$  gas ( $D = +1180\text{--}1400\ \mu\text{m}$ ,  $C = 7.68\ \text{mol}\cdot\text{L}^{-1}$ ,  $\text{SS} = 400\ \text{rpm}$ ,  $S/L = 2/100\ \text{g}\cdot\text{mL}^{-1}$ ).

**3.5. Effect of Stirring Speed.** Experiments were also conducted to investigate the effect of the stirring speed on the reaction rate, employing the speeds of 300, 400, 500, and 600 rpm. The experiments were carried out using the  $+1180\text{--}1400\ \mu\text{m}$  sample at  $45\ ^\circ\text{C}$ . The ammonia concentration was  $7.68\ \text{mol}\cdot\text{L}^{-1}$  and the solid-to-liquid ratio was  $2/100\ \text{g}\cdot\text{mL}^{-1}$ . The dissolution values at 600 rpm were almost the same as those at 500 rpm. For this reason, these values were not plotted and not used in kinetics evaluations. It was observed that the leaching rate increased gradually with increasing stirring speed, as shown in Figure 7.

#### 4. Kinetic Analysis

Fluid–solid reactions are numerous and of great industrial importance. In the leaching processes of ores with solutions, solid particles do not appreciably change in size during the heterogeneous reaction if the ore contains large amounts of impurities that remain as a nonflaking ash. In this kind of reactions, there are some physical steps that can affect the rate of the process, in

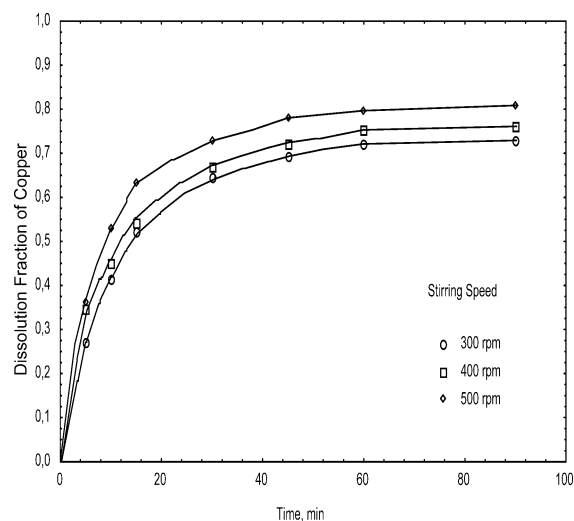


**Figure 7.** Effect of stirring speed on the leaching rate of malachite in water saturated with  $\text{NH}_3$  gas ( $D = +1180\text{--}1400\ \mu\text{m}$ ,  $T = 45\ ^\circ\text{C}$ ,  $C = 7.68\ \text{mol}\cdot\text{L}^{-1}$ ,  $S/L = 2/100\ \text{g}\cdot\text{mL}^{-1}$ ).

addition to the chemical reaction, such as diffusion through the fluid film and/or inert solid layer of the reactant or product.

The most important models suggested for the derivation of the rate expression of a noncatalytic fluid–solid reaction are the shrinking core model and the progressive conversion model.

According to the shrinking core model, it is thought that the reaction takes place on the outer surface of the solid and that this surface shrinks toward the center of the solid as the reaction proceeds, leaving behind an inert solid layer, called the “ash layer”, around the unreacted shrinking core.<sup>16</sup>

According to this model, in the solid–liquid reaction



If the reaction rate is controlled by diffusion through the ash layer consisting of the insoluble part around the unreacted core, the integrated rate expression is as follows

$$1 - 3(1 - X_B)^{2/3} + 2(1 - X_B) = \frac{6bD_e C_A t}{\rho_B R^2} = \frac{t}{t^*} \quad (10)$$

If the reaction rate is controlled by the surface chemical reaction, then the integrated rate expression becomes

$$1 - (1 - X_B)^{1/3} = \frac{bk_s C_A t}{\rho_B R} = \frac{t}{t^*} \quad (11)$$

If the reaction rate is controlled by diffusion through the liquid film, the integrated rate expression becomes

$$X_B = \frac{3bk_g C_A t}{\rho_B R} = \frac{t}{t^*} \quad (12)$$

where  $X_B$  is the conversion fraction of solid.

According to the progressive conversion model, the reaction can agree various models, called pseudo-homogen models, such as first order, second order, etc. For



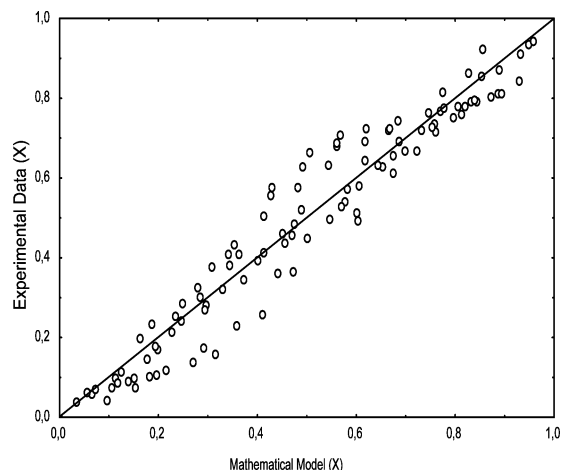


**Figure 8.** Comparison of mathematical model with experimental data.

example, if the reaction rate conforms with a pseudo-first-order model, the rate equation is

$$\frac{dX_B}{dt} = k(X_B) \quad (13)$$

If the reaction rate conforms with a pseudo-second-order model, the rate equation is

$$\frac{dX_B}{dt} = k(1 - X_B) \quad (14)$$

The results obtained with various parameters were used in the investigation of the leaching kinetics of malachite. Although the leaching experiments were carried out for up to 90-min reaction periods, the data for only the first 60 min were used in the kinetics calculations because the leaching did not proceed after 60 min. The effect of the ammonia concentration on the leaching rate was examined by using various ratios of  $\text{NH}_3\text{-N}_2$  mixtures. In the deviation of the mathematical model for this system,  $\text{NH}_3$  concentration for each temperature was determined from the plot of concentration versus temperature given in Figure 2. Thus, the effect of temperature on the leaching rate was taken into account with concentration changes in the kinetics calculations.

In investigating the effect of particle size on the leaching rate, the particle sizes were taken as arithmetic averages of two consecutive sieve sizes used in the particle size fraction. For the kinetic analysis, various reaction models were tested statistically, and it was thought that the leaching rate could be expressed with a model as follows

$$f(X) = kD^g C^a (S/L)^c (SS)^d e^{-(E/RT)} t^e \quad (15)$$

and it was determined that the best equation representing the leaching process was a pseudo-second-order model

$$\frac{X}{1-X} = 20.985 D^{-0.64} C^{4.86} (S/L)^{-0.59} (SS)^{1.25} e^{-(85.160/RT)} t^{0.76} \quad (16)$$

The correlation coefficient calculated for this regression was 0.97. A plot of the experimental values of the conversion factors versus those from the mathematical

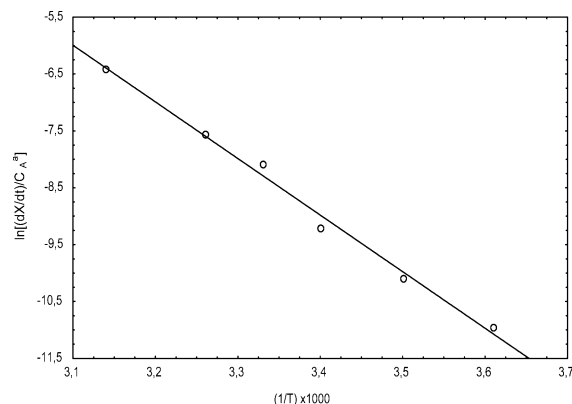


**Figure 9.** Arrhenius plot in accordance with the initial reaction rates from Figure 6.

model given in Figure 8 shows that the model is quite acceptable for this system.

To check the accuracy of the activation energy found statistically, the activation energy was also calculated by the Arrhenius equation using initial rates from the graphs of the leached fraction versus time in Figure 6. The Arrhenius plot in accordance with the initial reaction rates is shown in Figure 9. The initial rates were predicted by taking into account the first 3% of the leaching<sup>17</sup>

$$\text{initial reaction rate} = \frac{dX}{dt} \approx \frac{\Delta X}{\Delta t} \quad (17)$$

where  $\Delta x$  is the 3% leaching amount and  $\Delta t$  is the time required for 3% leaching. The ammonia concentration in the aqueous solution changes with temperature. To eliminate the effect of this change on the leaching rate constant,  $k$ , eq 18 was written

$$\frac{dX}{dt} = kC^a \quad (18)$$

$$\left(\frac{dX}{dt}\right)_{t=0} = k C^a \quad (19)$$

$$\ln \left[ \frac{\left(\frac{dX}{dt}\right)_{t=0}}{C^a} \right] = \ln k = \ln(k_0 e^{-(E/RT)}) \quad (20)$$

$$\ln k = \ln k_0 - \left(\frac{E}{R}\right) \left(\frac{1}{T}\right) \quad (21)$$

From the plot of  $\ln k$  versus  $1/T$  constructed by eq 21 taking into account, the activation energy was found to be  $85.16 \text{ kJ}\cdot\text{mol}^{-1}$  and the Arrhenius constant,  $k_0$ , to be  $8.23 \times 10^{10}$ . This value of the activation energy was the same as that found statistically.

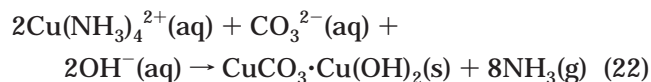
## 5. Conclusions

A kinetic study was conducted to understand the leaching mechanism of malachite in  $\text{NH}_3$ -saturated water. It was determined that malachite was dissolved completely in  $\text{NH}_3$ -saturated water and this process is convenient way for recovering copper from malachite. The leaching rate increased with decreasing particle size and solid-to-liquid ratio and with increasing ammonia concentration, temperature, and stirring speed.

The leaching rate of malachite was found to increase with increasing  $\text{NH}_3$  concentration. Even though the solubility of  $\text{NH}_3$  in water decreases with temperature, the increase of the leaching rate with increasing temperature shows that the temperature is much more effective on the leaching rate than the ammonia concentration. The stirring speed dependency of the leaching rate implied that the leaching rate of malachite was controlled by the removal of the  $\text{Cu}(\text{NH}_3)_4^{2+}$  complex from the malachite lattice.<sup>5</sup>

It was found that the leaching rate conforms with pseudo-second-order kinetics with an activation energy of  $85.16 \text{ kJ}\cdot\text{mol}^{-1}$ . According to the model, the stirring speed is one of the most effective parameters. As the stirring speed rose, malachite in gangue materials, which basically consists of  $\text{SiO}_2$ , reacted more rapidly. In addition, the gas-liquid interface increases with increasing stirring speed, and the removal of the reaction products from the interface is promoted.<sup>18</sup> The activation energy value indicates that the proposed mechanism is reasonable.

Malachite and  $\text{NH}_3$  from the leaching solutions can be recovered by steam stripping of the solution or by boiling of the solution as follows



and ammonia can be recycled in the leaching system.

As a result, it was determined that ammonia was a more appropriate leachant for copper in oxidized ores than sulfuric acid for many reasons, such as its selectivity for copper in oxidized copper ores, the recovery of pure malachite precipitate and ammonia by steam stripping, and the recycling of ammonia in the process.

## Nomenclature

A = liquid reactant  
 B = solid reactant  
 a = power of concentration in the rate expression  
 b = stoichiometric coefficient of B (solid) reacting with each mole of A (fluid)  
 c = power of the solid-to-liquid ratio in the rate expression  
 d = power of the stirring speed in the rate expression  
 e = power of the chemical reaction time in the rate expression  
 g = power of the particle size in the rate expression  
 C = ammonia concentration in water ( $\text{mol}\cdot\text{L}^{-1}$ )  
 D = particle size ( $\mu\text{m}$ )  
 $D_e$  = diffusivity of ions through the ash layer ( $\text{m}^2\cdot\text{s}^{-1}$ )  
 E = activation energy ( $\text{kJ}\cdot\text{mol}^{-1}$ )  
 k = chemical reaction rate constant  
 $k_0$  = Arrhenius constant ( $\text{s}^{-1}$ )  
 $k_s$  = surface chemical reaction rate constant ( $\text{s}^{-1}$ )  
 L = amount of liquid (kg)  
 R = particle radius (m)  
 S = amount of solid (kg)  
 S/L = solid-to-liquid ratio ( $\text{g}\cdot\text{mL}^{-1}$ )

SS = stirring speed (rpm)

T = temperature ( $^{\circ}\text{C}$ )

t = time (min)

$t^*$  = time for complete conversion of single solid particle (min)

X = leaching fraction of Cu

$X_B$  = leaching fraction of B,  $(C_{B0} - C_B)/C_{B0}$

$\rho_B$  = solid density ( $\text{g}\cdot\text{L}^{-1}$ )

## Literature Cited

- (1) Biswas, A. K.; Davenport, W. G. *Extractive Metallurgy of Copper*; Pergamon Press: Oxford, U.K., 1980.
- (2) Greenawalt, W. E. *Trans. Am. Inst. Min.* **1974**, *70*, 148.
- (3) Chase, C. K. The Ammonia Leach for Copper Recovery, Leaching Recovering Copper As-Mined Material. In *Proceedings of the Las Vegas Symposium*; AIME: New York, 1980; pp 95–103.
- (4) Jackson, E. *Hydrometallurgical Extraction and Reclamation*; Ellis Harwood Ltd.: Chichester, U.K., 1986.
- (5) Awakura, Y.; Hirato, T.; Kagawa, A.; Yamada, Y.; Majima, H. Dissolution of Malachite in Aqueous Ethylenediaminetetraacetate Solution. *Metall. Trans. B* **1991**, *22*, 569–574.
- (6) Çolak, S.; Çakıcı, A.; Ekinci, Z.; Atakül, H. Dissolution Kinetics of Malachite in Water Saturated with Sulphur Dioxide. *Chim. Acta Turc.* **1994**, *22*, 315–325.
- (7) Yartaşı, A.; Çopur, M. Dissolution Kinetics of Copper(II) Oxide in Ammonium Chloride Solutions. *Min. Eng.* **1996**, *9* (6), 639–698.
- (8) Künkül, A.; Kocakerim, M. M.; Yapıcı, S.; Demirbağ, A. Leaching Kinetics of Malachite in Ammonia Solutions. *Int. J. Min. Process.* **1994**, *41*, 167–182.
- (9) Oudenne, P. D.; Olson, F. A. Leaching Kinetics of Malachite in Ammonium Carbonate Solutions. *Metall. Trans. B* **1983**, *14*, 33–40.
- (10) Konishi, Y.; Katoh, M.; Asai, S. Leaching Kinetics of Copper From Natural Chalcocite in Alkaline  $\text{Na}_4\text{EDTA}$  Solutions. *Metall. Trans. B* **1991**, *22*, 295–320.
- (11) Ekmekyapar, A.; Oya, R.; Künkül, A. Dissolution Kinetics of an Oxidized Copper Ore in Ammonium Chloride Solution. *Chem. Biochem. Eng.* **2003**, *17* (4), 261–266.
- (12) Ekmekyapar, A.; Çolak, S.; Alkan, M. Dissolution Kinetics of Oxidized Copper Ore in Water Saturated by Chlorine. *J. Chem. Technol. Biotechnol.* **1988**, *43*, 195–204.
- (13) Bingöl, D.; Canbazoglu, M. Dissolution Kinetics of Malachite in Sulphuric Acid. *Hydrometallurgy* **2004**, *72*, 159–165.
- (14) Tamura, H.; Ito, N.; Kitano, M.; Takasaki, S. A Kinetic Model of The Dissolution of the Copper(II) Oxide in EDTA Solutions Considering The Coupling of Metal and Oxide Ion Transfer. *Corros. Sci.* **2001**, *43*, 1675–1691.
- (15) Gülensoy, H. *Basis of Complexometry and Complexometric Titrations*; Istanbul University Publishings: Istanbul, Turkey, 1984.
- (16) Levenspiel, O. *Chemical Reaction Engineering*; Wiley: New York, 1972.
- (17) Petrucci, R. H. *General Chemistry Principles and Modern Applications*; Macmillan Publishing Company: New York, 1985.
- (18) Tozawa, K.; Umetsu, Y.; Sato, K. On chemistry of ammonia leaching of copper concentrate. In *Extractive Metallurgy of Copper*; Yannopoulos, J. C., Agarwal, J. C., Eds.; AIME: New York, 1976; Vol. II, pp 706–721.

Received for review November 17, 2003

Revised manuscript received April 8, 2004

Accepted May 23, 2004

IE0342558